Punjab University Journal of Mathematics (2024), 56(9), 543-566
https://doi.org/10.52280/pujm.2024.56(9)04

Dynamic Analysis of the (2+1)-Dimensional Zoomeron Model Using Advanced Analytical Techniques

Alisha Javed[1], Umair Asghar[2*], Muhammad Imran Asjad[1]
[1] *Department of Mathematics, University of Management and Technology, Lahore, Pakistan,*
[2] *Department of Mathematics and Statistics, University of Lahore, Lahore, Pakistan*
Email: umairas926@gmail.com

Received: 11 December, 2024 / Accepted: 07 April, 2025 / Published online: 14 April, 2025

Abstract. In this paper, we investigate a nonlinear partial differential equation (NLPDE) known as the (2+1)-D Zoomeron model. This model is widely used in fluid dynamics, SONAR (Sound Navigation and Ranging) systems, optical fiber communication, and various other mathematical, physical, and technological fields. The exact solutions are obtained with the help of two advanced methodologies, the Sardar sub-equation technique and a new extended algebraic technique, that can offer a variety of soliton solutions with unique dynamic characteristics. These methodologies are efficient in understanding the complex behavior of the model. Traveling wave solutions are obtained in the paper with the help of Mathematica software, to explain a sound and effective new mathematical approach. The generated solutions cover a wide range of phenomena. These techniques give results in the form of plane wave solutions, hyperbolic solutions, periodic solutions, mixed periodic solutions, shock wave solutions, exponential solutions, and trigonometric solutions. Moreover, to understand the behavior of the obtained results, draw it in 3D, 2D as well, and contour from. The research outcomes increase the model's accuracy and demonstrate the new concept's value in learning technical physical systems. The next study in the domains of theoretical physics and applied mathematics is made possible by this work.

AMS (MOS) Subject Classification Codes: 35Q51; 35C07; 25U09; 35Q53
Key Words: (2+1)-D Zoomeron model; Sardar sub-equation technique; New extended direct algebraic approach; Exact solutions; Non-linear partial differential equation (NLPDEs).

1. Introduction

Solitons are an interesting phenomenon in nonlinear science. They occur due to the delicate interaction of a medium's dispersive and nonlinear properties. Solitary waves can arise as a result of nonlinear effects, which enable waves to interact, and dispersive effects, which cause waves of various frequencies to move at different speeds, can counteract dispersion and keep the soliton's shape as it propagates [26, 19]. In the context of optical fibers, solitons are solitary waves that propagate through the fiber while retaining their amplitude and shape [8]. Solitons offer an effective solution to signal deterioration in long-distance underwater communications [14]. Additionally, SONAR (Sound Navigation and Ranging) systems may find use for solitons. SONAR systems use sound waves to detect and locate objects underwater [17]. In optical fiber and telecommunication systems [39, 4, 2].

To find the exact solutions various techniques are utilized. Many different kinds of nonlinear problems have developed in the field of nonlinear science, featuring models such as He's Variational Method [27], the (F-expansion) method [30], Hirota bilinear forms [24], the new extended generalized Kudryashov method [41], and the 1^{st} Integral Method [43]. Utilizing the extended tanh-function technique [40], Semi-analytical methods [5], the function method [15], new auxiliary method [6], simple direct method [23], the $(\frac{1}{G'})$ technique [11], Lie symmetry analysis [21], tanh method [38], bilinear residual network method [45], modified auxiliary equation method [20], bilinear neural network [44], $\frac{G}{G'}$ methodology [13], Jacobi elliptic function method [32], homogeneous balance method [29], the Miura transformation [22], cubic B-spline [28] and Wronskian determinant technique [33]. These methods provide exact soliton solutions, offering insights into the model's behavior across various scenarios. Techniques such as the Bäcklund Transformations, Hirota's Direct Method, and the Inverse Scattering Transform allow for a thorough investigation of soliton dynamics in a variety of mathematical and physical contexts [25, 46, 31, 1].

In this manuscript, to obtain the exact soliton solutions two methodologies are applied. Namely, the Sardar sub-equation technique and the new extended direct algebraic approach. These models give results in the form of shock solutions, singular solutions, mixed complex solitary-shock solutions, mixed singular solutions, mixed shock-singular solutions, mixed trigonometric solutions, complex solutions, trigonometric solutions, mixed trigonometric solutions, periodic and mixed periodic solutions, single and mixed wave compositions, and mixed hyperbolic solutions. The Sardar sub-equation method includes four cases, each with five to six sets of conditions. The advantage of this technique is that it is easy to solve and gives exact solutions in some steps and these solutions also satisfy the original equation. The other model is a new extended direct algebraic method. It consists of twelve cases with different cases and each case has four to five numerous sets. This method is beneficial for both new and experienced investigators as it provides accurate solution solutions quickly and easily. Its effectiveness, simplicity of use, and accessibility enable fast understanding and analysis, offering insightful information in a variety of fields. The motivation for our outcomes is that it can be used in are often employed in systems for optical fiber communication. Here are some applications and uses of our outcomes, in optical fiber communication, one of the primary benefits of solitons is their long-range shape and intensity maintenance, which allows for reliable information transfer. Results are employed in water wave and optical systems, and they can also occur in some kinds of sound systems. Also helpful in SONAR systems, which use sound waves for underwater navigation and detection. Certain ideas on nonlinear wave propagation and solitons may have an impact on the development and functionality of cutting-edge SONAR systems.

The paper is divided into different sections. In Section 2, we explain the analytical method and explore some beneficial factors of the new extended direct algebraic technique and Sardar sub-equation method. Section 3 focuses on developing solitary wave solutions, accompanied by a clear graphic representation. Moving on to Section 4, to present and discuss the results. The final part of the paper is a conclusion summarising the entire research.

2. Governing Model

A focus of research is the (2+1)-D Zoomeron model, which presents an extensive array of nonlinear dynamics that resist considered mathematical models. soliton solution of the (2+1)-dimensional Zoomeron equation [18]. Mathematical methods for a reliable treatment. By exposing the interactions between the velocities of solitons generated for this equation and the impacts of gradient flow directions, it seeks to obtain a physically distinct viewpoint. Furthermore, with the assistance of bilinear formalism, a direct method is utilized for obtaining solitary wave and rogue wave solutions employing certain auxiliary functions [10]. As such, there have simply been two different types of solitons. The first is called an accelerated soliton, which originates from one side in a distant time and returns to that side at the same speed in the distant future. The second was a trapped soliton, which oscillated repeatedly in the same direction around a fixed point in space. Boomeron was the first, and Trappon was the second. This led to the derivation of the classical Zoomeron equation [16]. The non-linear partial differential Zoomeron equation is,

$$\left(\frac{\mathbf{F}_{xy}}{\mathbf{F}}\right)_{tt} - \left(\frac{\mathbf{F}_{xy}}{\mathbf{F}}\right)_{xx} + 2\left(\mathbf{F}^2\right)_{xt} = 0, \tag{2. 1}$$

were, $\mathbf{F}(\mathbf{x}, \mathbf{y}, \mathbf{t})$ represents the magnitude of a soliton, x, and y denote the positional components, and t represents the time component. In this study, we execute an in-depth examination of the (2+1)-D Zoomeron equation, utilising new mathematical methods to identify the complex solutions that emerge in this enlarged framework. Our intention is to make an important addition to the rapidly evolving field of nonlinear dynamics by providing both theoretical understanding of the behaviour of waves and solitons and prospective applications in a variety of interdisciplinary fields. We seek to learn more about dynamic systems in higher dimensions and discover new aspects of nonlinear processes as we work through the difficulties of the (2+1)-D Zoomeron equation [37].

3. Representation of the analytical methods

The suggested approach is efficaciously relevant to complex non-linear utilize systems:

$$\mathcal{A}(\mathbf{F}, \mathbf{F}_x, \mathbf{F}_t, \mathbf{F}_{xt}, \mathbf{F}_{xx}, ...) = 0, \tag{3. 2}$$

where, $\mathcal{A}$ is the polynomial function in $\mathbf{F}$, and $\mathbf{F}(x, t)$is in fact an undefined function. Its impartial variables are temporal and spatial.

$$\mathcal{C}(\mathbb{K}, \mathbb{K}', \mathbb{K}'', ...) = 0. \tag{3. 3}$$

By simply taking the use of the given transformation:

$$\mathbf{F}(x, t) = \mathbb{K}(\delta), \tag{3. 4}$$

were, $\delta = \psi x - \phi t$.
To set up a travelling wave transformation to reap the effects of Eq. (2. 1).

$$\mathbf{F}(x,t) = \mathbb{K}(\delta),\ \delta = x + \epsilon_0 y - \epsilon_1 t. \tag{3. 5}$$

where, ϵ_0 is constant and ϵ_0 is wave speed. Applying the formerly mentioned travelling wave transformation inside Eq. (3. 2), and get the ODE,

$$\epsilon_0\left(\epsilon_1^2 - 1\right)\mathbb{K}^{''} - 2\epsilon_1\mathbb{K}^3 - Q\mathbb{K} = 0. \tag{3. 6}$$

3.1. **Sardar sub-equation method.** Consider Eq. (3. 3) have the solutions as follow [3, 35]:

$$\mathbb{V}(\zeta) = \sum_{j=0}^{M}\left[\Lambda_j \Omega^j(\zeta)\right], \tag{3. 7}$$

where $\Lambda_j(0 \le j \le M)$ are constants.

$$(\Omega^{'}(\zeta))^2 = G + F\Omega^2(\zeta) + \Omega^4(\zeta)), \tag{3. 8}$$

where G and F are real constants and Eq.(3. 8) yields the sets of solutions as:

Case 1: When $F > 0$ and $G = 0$, then

$$\Omega_1^{\pm}(\zeta) = \pm\sqrt{-Fpq}sech_{pq}(\sqrt{F}\zeta), \tag{3. 9}$$

$$\Omega_2^{\pm}(\zeta) = \pm\sqrt{-Fpq}csc_{pq}(\sqrt{F}\zeta), \tag{3. 10}$$

where,

$$sech_{pq}(\zeta) = \frac{2}{pe^{\zeta} + qe^{\zeta}}, csch_{pq}(\zeta) = \frac{2}{pe^{\zeta} + qe^{\zeta}}. \tag{3. 11}$$

Case 2: When $F < 0$ and $G = 0$, then

$$\Omega_3^{\pm}(\zeta) = \pm\sqrt{-Fpq}sech_{pq}(\sqrt{-F}\zeta), \tag{3. 12}$$

$$\Omega_4^{\pm}(\zeta) = \pm\sqrt{-Fpq}csc_{pq}(\sqrt{-F}\zeta), \tag{3. 13}$$

where,

$$sech_{pq}(\zeta) = \frac{2}{pe^{i\zeta} + qe^{-i\zeta}}, csch_{pq}(\zeta) = \frac{2_i}{pe^{i\zeta} + qe^{-i\zeta}}. \tag{3. 14}$$

Case 3: When $F < 0$ and G=$\frac{a^2}{4b}$ then,

$$\Omega_5^{\pm}(\zeta) = \pm\sqrt{-\frac{F}{2}}tanh_{pq}(\sqrt{-\frac{F}{2}}\zeta), \tag{3. 15}$$

$$\Omega_6^{\pm}(\zeta) = \pm\sqrt{-\frac{F}{2}}coth_{pq}(\sqrt{-\frac{F}{2}}\zeta), \tag{3. 16}$$

$$\Omega_7^{\pm}(\zeta) = \pm\sqrt{-\frac{F}{2}}(tanh_{pq}(\sqrt{-2F}\zeta) \pm i\sqrt{pq}sech_pq(\sqrt{-2F\zeta})), \tag{3. 17}$$

$$\Omega_8^{\pm}(\zeta) = \pm\sqrt{-\frac{F}{2}}(coth_{pq}(\sqrt{-2F}\zeta) \pm i\sqrt{pq}csch_{pq}(\sqrt{-2F\zeta})), \tag{3. 18}$$

$$\Omega_9^{\pm}(\zeta) = \pm\sqrt{-\frac{F}{8}}(tanh_{pq}(\sqrt{-\frac{F}{8}}\zeta) + coth_pq(\sqrt{-\frac{F}{8}}\zeta)), \tag{3. 19}$$

where,

$$tanh_{pq}(\zeta) = \frac{pe^{\zeta} - qe^{-\zeta}}{pe^{\zeta} + qe^{-\zeta}}, coth_{pq}(\zeta) = \frac{pe^{\zeta} + qe^{-\zeta}}{pe^{\zeta} - qe^{-\zeta}}. \tag{3. 20}$$

Case 4: When $F > 0$ and G=$\frac{a^2}{4}$ then,

$$\Omega_{10}^{\pm}(\zeta) = \pm\sqrt{\frac{F}{2}}tanh_{pq}(\sqrt{\frac{F}{2}}\zeta), \tag{3. 21}$$

$$\Omega_{11}^{\pm}(\zeta) = \pm\sqrt{\frac{F}{2}}cot_{pq}(\sqrt{\frac{F}{2}}\zeta), \tag{3. 22}$$

$$\Omega_{12}^{\pm}(\zeta) = \pm\sqrt{\frac{F}{2}}(tan_{pq}(\sqrt{2F}\zeta) \pm \sqrt{pq}sec_{pq}(\sqrt{2F\zeta})), \tag{3. 23}$$

$$\Omega_{13}^{\pm}(\zeta) = \pm\sqrt{\frac{F}{2}}(cot_{pq}(\sqrt{2F}\zeta) \pm \sqrt{pq}csc_{pq}(\sqrt{2F\zeta})), \tag{3. 24}$$

$$\Omega_{14}^{\pm}(\zeta) = \pm\sqrt{\frac{F}{8}}((tan_{pq}(\sqrt{\frac{F}{8}}\zeta) + cot_{pq}(\sqrt{\frac{F}{8}}\zeta)), \tag{3. 25}$$

where,

$$tan_{pq}(\zeta) = -i\frac{pe^{i\zeta} - qe^{-i\zeta}}{pe^{i\zeta} + qe^{-i\zeta}}, cot_{pq}(\zeta) = i\frac{pe^{i\zeta} + qe^{-i\zeta}}{pe^{i\zeta} - qe^{-i\zeta}}. \tag{3. 26}$$

3.1.1. *Applications of Sardar sub-equation Method:* To achieve the soliton wave structures of (2+1) D Zoomeron Model, the SSM is applied on Eq. (3. 6). By balance rule on terms of $\mathbb{K}^{''}$ and $\mathbb{K}^3$ in Eq. (3. 6), gives $Q = 1$, so Eq. (3. 7) changes to

$$V(\zeta) = e_0 + e_1\Omega(\zeta), \tag{3. 27}$$

where e_0, e_1 are constants. Replacing the Eq.(3. 27) along with Eq. (3. 8) into Eq. (3. 6), and gets the set of equations in ϵ_0, ϵ_1, and Q. On resolving the system of equations, to attain

$$Q = F\epsilon_0(\epsilon_1^2 - 1), e_0 = 0, e_1 = \pm\sqrt{\frac{\epsilon_0(\epsilon_1^2 - 1)}{\epsilon_1}}. \tag{3. 28}$$

Case 1: When $F > 0$ and $G = 0$ then,

$$\mathbb{K}_1^{\pm}(x,y,t) = \pm\sqrt{\frac{\epsilon_0(\epsilon_1^2-1)}{\epsilon_1}} \pm \sqrt{-Fpq}sech_{pq}(\sqrt{F}\zeta), \tag{3. 29}$$

$$\mathbb{K}_2^{\pm}(x,y,t) = \pm\sqrt{\frac{\epsilon_0(\epsilon_1^2-1)}{\epsilon_1}} \pm \sqrt{-Fpq}csc_{pq}(\sqrt{F}\zeta). \tag{3. 30}$$

Case 2: When $F < 0$ and $G = 0$ then,

$$\mathbb{K}_3^{\pm}(x,y,t) = \pm\sqrt{\frac{\epsilon_0(\epsilon_1^2-1)}{\epsilon_1}} \pm \sqrt{-Fpq}sech_{pq}(\sqrt{-F}\zeta), \tag{3. 31}$$

$$\mathbb{K}_4^{\pm}(x,y,t) = \pm\sqrt{\frac{\epsilon_0(\epsilon_1^2-1)}{\epsilon_1}} \pm \sqrt{-Fpq}csc_{pq}(\sqrt{-F}\zeta). \tag{3. 32}$$

Case 3: When $F < 0$ and G=$\frac{a^2}{4b}$ then,

$$\mathbb{K}_5^{\pm}(x,y,t) = \pm\sqrt{\frac{\epsilon_0(\epsilon_1^2-1)}{\epsilon_1}} \pm \sqrt{-\frac{F}{2}}tanh_{pq}(\sqrt{-\frac{F}{2}}\zeta), \tag{3. 33}$$

$$\mathbb{K}_6^{\pm}(x,y,t) = \pm\sqrt{\frac{\epsilon_0(\epsilon_1^2-1)}{\epsilon_1}} \pm \sqrt{-\frac{F}{2}}coth_{pq}(\sqrt{-\frac{F}{2}}\zeta), \tag{3. 34}$$

$$\mathbb{K}_7^{\pm}(x,y,t) = \pm\sqrt{\frac{\epsilon_0(\epsilon_1^2-1)}{\epsilon_1}} \pm i\sqrt{pq}sech_p q(\sqrt{-2F\zeta})), \tag{3. 35}$$

$$\mathbb{K}_8^{\pm}(x,y,t) = \pm\sqrt{\frac{\epsilon_0(\epsilon_1^2-1)}{\epsilon_1}} \pm i\sqrt{pq}csch_{pq}(\sqrt{-2F\zeta})), \tag{3. 36}$$

$$\mathbb{K}_9^{\pm}(x,y,t) = \pm\sqrt{\frac{\epsilon_0(\epsilon_1^2-1)}{\epsilon_1}} \pm (\sqrt{-\frac{F}{8}}(tanh_{pq}(\sqrt{-\frac{F}{8}}\zeta) + coth_p q(\sqrt{-\frac{F}{8}}\zeta))) \tag{3. 37}$$

Case 4: When $F > 0$ and G=$\frac{a^2}{4}$ then,

$$\mathbb{K}_{10}^{\pm}(x,y,t) = \pm\sqrt{\frac{\epsilon_0(\epsilon_1^2-1)}{\epsilon_1}} \pm \sqrt{\frac{F}{2}}tanh_{pq}(\sqrt{\frac{F}{2}}\zeta), \tag{3. 38}$$

$$\mathbb{K}_{11}^{\pm}(x,y,t) = \pm\sqrt{\frac{\epsilon_0(\epsilon_1^2-1)}{\epsilon_1}} \pm \sqrt{\frac{F}{2}}cot_{pq}(\sqrt{\frac{F}{2}}\zeta), \tag{3. 39}$$

$$\mathbb{K}_{12}^{\pm}(x,y,t) = \pm\sqrt{\frac{\epsilon_0(\epsilon_1^2-1)}{\epsilon_1}} \pm (\sqrt{\frac{F}{2}}(tan_{pq}(\sqrt{2F}\zeta) \pm \sqrt{pq}sec_{pq}(\sqrt{2F\zeta}))), \quad (3.\ 40)$$

$$\mathbb{K}_{13}^{\pm}(x,y,t) = \pm\sqrt{\frac{\epsilon_0(\epsilon_1^2-1)}{\epsilon_1}} \pm (\sqrt{\frac{F}{2}}(cot_{pq}(\sqrt{2F}\zeta) \pm \sqrt{pq}csc_{pq}(\sqrt{2F\zeta}))), \quad (3.\ 41)$$

$$\mathbb{K}_{14}^{\pm}(x,y,t) = \pm\sqrt{\frac{\epsilon_0(\epsilon_1^2-1)}{\epsilon_1}} \pm (\sqrt{\frac{F}{8}}((tan_{pq}(\sqrt{\frac{F}{8}}\zeta) + cot_{pq}(\sqrt{\frac{F}{8}}\zeta))). \quad (3.\ 42)$$

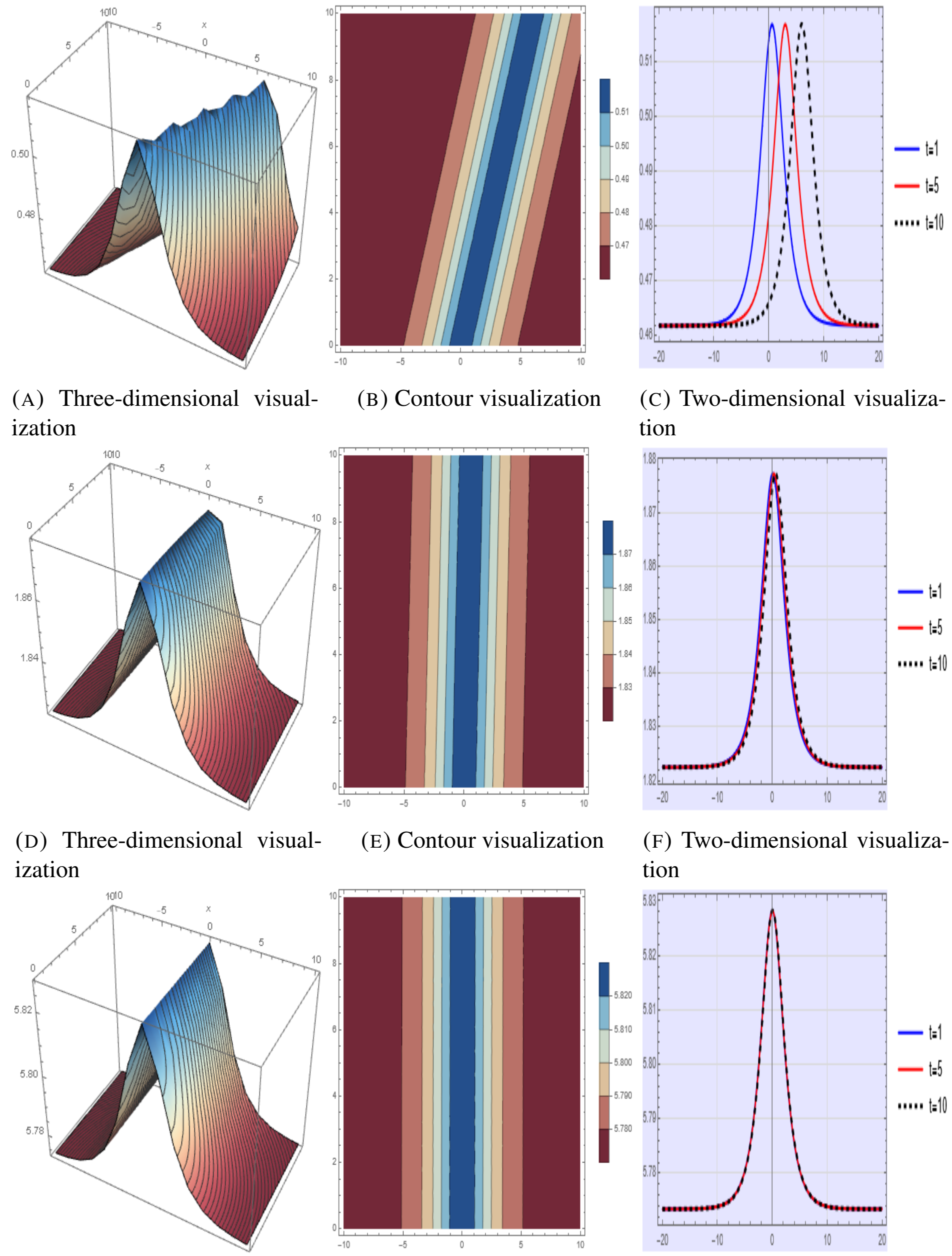

(A) Three-dimensional visualization

(B) Contour visualization

(C) Two-dimensional visualization

(D) Three-dimensional visualization

(E) Contour visualization

(F) Two-dimensional visualization

(G) Three-dimensional visualization

(H) Contour visualization

(I) Two-dimensional visualization

FIGURE 1. The solution $\mathbb{K}_1(x, y, t)$ is represented in 3D ,2D and contour plot.

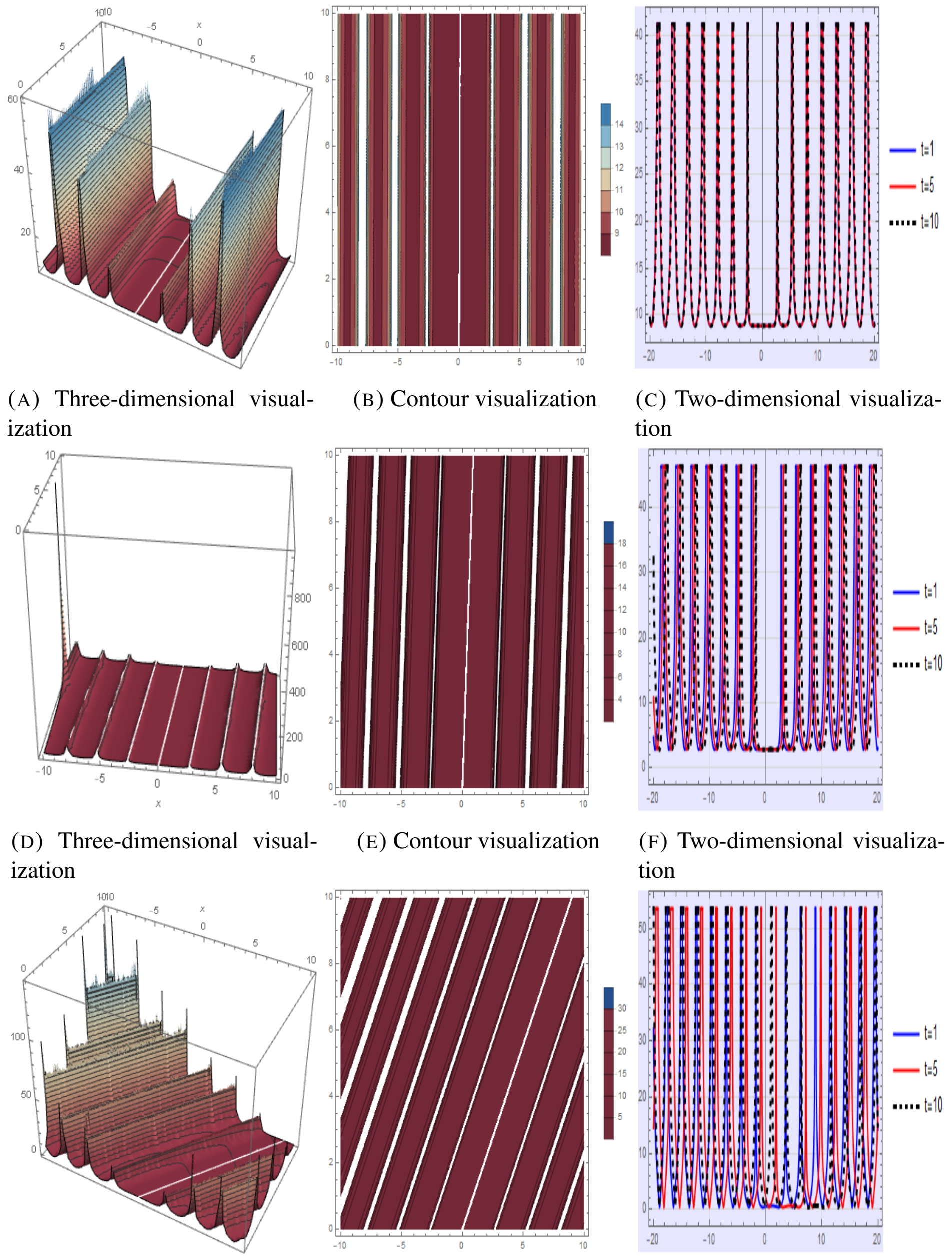

(A) Three-dimensional visualization (B) Contour visualization (C) Two-dimensional visualization

(D) Three-dimensional visualization (E) Contour visualization (F) Two-dimensional visualization

(G) Three-dimensional visualization (H) Contour visualization (I) Two-dimensional visualization

FIGURE 2. The solution of $\mathbb{K}_{13}(x, y, t)$ is represented in 3D, 2D, and contour plots.

3.2. **New extended direct algebraic method.** Suppose that Eq. (3. 3) has the solution of the form given in Eq. (3. 4) [7, 12],

$$\mathbb{K}(\delta)=\sum_{i=0}^{n}\left[r_i(\mathbb{Z}(\delta))^i\right], \tag{3. 43}$$

and

$$\mathbb{Z}'(\delta)=\ln[\varrho]\left(\alpha+ß\mathbb{Z}(\delta)+\ell\mathbb{Z}^2(\delta)\right),\ \varrho\neq(0,1), \tag{3. 44}$$

Eq. (3. 44) has extended roots in several families by selecting parameters where α, ß, and ℓ represent the actual values.

Group 1: When $ß^2-4\alpha\ell<0$, and $\ell\neq 0$,

$$\mathbb{Z}_1(\delta)=-\frac{ß}{2\ell}+\frac{\sqrt{-\mathfrak{X}}}{2\ell}\tan_\varrho\left(\frac{\sqrt{-\mathfrak{X}}}{2}\delta\right), \tag{3. 45}$$

$$\mathbb{Z}_2(\delta)=-\frac{ß}{2\ell}-\frac{\sqrt{-\mathfrak{X}}}{2\ell}\cot_\varrho\left(\frac{\sqrt{-\mathfrak{X}}}{2}\delta\right), \tag{3. 46}$$

$$\mathbb{Z}_3(\delta)=-\frac{ß}{2\ell}+\frac{\sqrt{-\mathfrak{X}}}{2\ell}\left(\tan_\varrho\left(\sqrt{-\mathfrak{X}}\delta\right)\pm\sqrt{mn}\sec_\varrho\left(\sqrt{-\mathfrak{X}}\delta\right)\right), \tag{3. 47}$$

$$\mathbb{Z}_4(\delta)=-\frac{ß}{2\ell}+\frac{\sqrt{-\mathfrak{X}}}{2\ell}\left(\cot_\varrho\left(\sqrt{-\mathfrak{X}}\delta\right)\pm\sqrt{mn}\csc_\varrho\left(\sqrt{-\mathfrak{X}}\delta\right)\right), \tag{3. 48}$$

$$\mathbb{Z}_5(\delta)=-\frac{ß}{2\ell}+\frac{\sqrt{-\mathfrak{X}}}{4\ell}\left(\tan_\varrho\left(\frac{\sqrt{-\mathfrak{X}}}{4}\delta\right)-\cot_\varrho\left(\frac{\sqrt{-\mathfrak{X}}}{4}\delta\right)\right). \tag{3. 49}$$

Group 2: When $ß^2-4\alpha\ell>0$, and $\ell\neq 0$,

$$\mathbb{Z}_6(\delta)=-\frac{ß}{2\ell}-\frac{\sqrt{\mathfrak{X}}}{2\ell}\tanh_\varrho\left(\frac{\sqrt{\mathfrak{X}}}{2}\ell\right), \tag{3. 50}$$

$$\mathbb{Z}_7(\delta)=-\frac{ß}{2\ell}-\frac{\sqrt{\mathfrak{X}}}{2\ell}\coth_\varrho\left(\frac{\sqrt{\mathfrak{X}}}{2}\ell\right), \tag{3. 51}$$

$$\mathbb{Z}_8(\delta)=-\frac{ß}{2\ell}+\frac{\sqrt{\mathfrak{X}}}{2\ell}\left(-\tanh_\varrho\left(\sqrt{\mathfrak{X}}\delta\right)\pm i\sqrt{mn}sech_\varrho\left(\sqrt{\mathfrak{X}}\delta\right)\right), \tag{3. 52}$$

$$\mathbb{Z}_9(\delta)=-\frac{ß}{2\ell}+\frac{\sqrt{\mathfrak{X}}}{2\ell}\left(-\coth_\varrho\left(\sqrt{\mathfrak{X}}\delta\right)\pm\sqrt{mn}csch_\varrho\left(\sqrt{\mathfrak{X}}\delta\right)\right), \tag{3. 53}$$

$$\mathbb{Z}_{10}(\delta)=-\frac{ß}{2\ell}-\frac{\sqrt{\mathfrak{X}}}{4\delta}\left(\tanh_\varrho\left(\frac{\sqrt{\mathfrak{X}}}{4}\delta\right)+\coth_\varrho\left(\frac{\sqrt{\mathfrak{X}}}{4}\delta\right)\right). \tag{3. 54}$$

Group 3: When $\alpha\ell > 0$ and $ß = 0$,

$$\mathbb{Z}_{11}(\delta) = \sqrt{\frac{\alpha}{\ell}}\, tan_{\varrho}\left(\sqrt{\alpha\ell}\delta\right), \tag{3. 55}$$

$$\mathbb{Z}_{12}(\delta) = -\sqrt{\frac{\alpha}{\ell}}\, cot_{\varrho}\left(\sqrt{\alpha\ell}\delta\right), \tag{3. 56}$$

$$\mathbb{Z}_{13}(\delta) = \sqrt{\frac{\alpha}{\ell}}\left(\tan_{\varrho}\left(2\sqrt{\alpha\ell}\delta\right) \pm \sqrt{mn}\, sec_{\varrho}\left(2\sqrt{\alpha\ell}\delta\right)\right), \tag{3. 57}$$

$$\mathbb{Z}_{14}(\delta) = \sqrt{\frac{\alpha}{\ell}}\left(- cot_{\varrho}\left(2\sqrt{\alpha\ell}\delta\right) \pm \sqrt{mn}\,\csc_{\varrho}\left(2\sqrt{\alpha\ell}\delta\right)\right), \tag{3. 58}$$

$$\mathbb{Z}_{15}(\delta) = \frac{1}{2}\sqrt{\frac{\alpha}{\ell}}\left(\tan_{\varrho}\left(\frac{\sqrt{\alpha\ell}}{2}\delta\right) - \cot_{\varrho}\left(\frac{\sqrt{\alpha\ell}}{2}\delta\right)\right). \tag{3. 59}$$

Group 4: When $\alpha\ell < 0$ and $ß = 0$,

$$\mathbb{Z}_{16}(\delta) = -\sqrt{-\frac{\alpha}{\ell}}\tanh_{\varrho}\left(\sqrt{-\alpha\ell}\delta\right), \tag{3. 60}$$

$$\mathbb{Z}_{17}(\delta) = -\sqrt{-\frac{\alpha}{\ell}}\coth_{\varrho}\left(\sqrt{-\alpha\ell}\delta\right), \tag{3. 61}$$

$$\mathbb{Z}_{18}(\delta) = \sqrt{-\frac{\alpha}{\ell}}\left(-\tanh_{\varrho}\left(2\sqrt{-\alpha\ell}\delta\right) \pm i\sqrt{mn} sech_{\varrho}\left(2\sqrt{-\alpha\ell}\delta\right)\right), \tag{3. 62}$$

$$\mathbb{Z}_{19}(\delta) = \sqrt{-\frac{\alpha}{\ell}}\left(-\coth_{\varrho}\left(2\sqrt{-\alpha\ell}\delta\right) \pm \sqrt{mn} csch_{\varrho}\left(2\sqrt{-\alpha\ell}\delta\right)\right), \tag{3. 63}$$

$$\mathbb{Z}_{20}(\delta) = -\frac{1}{2}\sqrt{-\frac{\alpha}{\ell}}\left(\tanh_{\varrho}\left(\frac{\sqrt{-\alpha\ell}}{2}\delta\right) + \ coth_{\varrho}\left(\frac{\sqrt{-\alpha\ell}}{2}\delta\right)\right). \tag{3. 64}$$

Group 5: When $ß = 0$ and $\alpha = \ell$,

$$\mathbb{Z}_{21}(\delta) = \tan_{\varrho}(\alpha\ell), \tag{3. 65}$$

$$\mathbb{Z}_{22}(\delta) = -\cot_{\varrho}(\alpha\ell), \tag{3. 66}$$

$$\mathbb{Z}_{23}(\delta) = \tan_{\varrho}(2\alpha\ell) \pm \sqrt{mn}\sec_{\varrho}(2\alpha\ell), \tag{3. 67}$$

$$\mathbb{Z}_{24}(\delta) = -\cot_{\varrho}(2\alpha\ell) \pm \sqrt{mn}\csc_{\varrho}(2\alpha\ell), \tag{3. 68}$$

$$\mathbb{Z}_{25}(\delta)=\frac{1}{2}\left(\tan_{\varrho}\left(\frac{\alpha}{2}\delta\right)-\cot_{\varrho}\left(\frac{\alpha}{2}\delta\right)\right). \tag{3. 69}$$

Group 6: When $ß=0$ and $\ell=-\alpha$,

$$\mathbb{Z}_{26}(\delta)=-\tanh_{\varrho}\left(\alpha\delta\right), \tag{3. 70}$$

$$\mathbb{Z}_{27}(\delta)=-\coth_{\varrho}\left(\alpha\delta\right), \tag{3. 71}$$

$$\mathbb{Z}_{28}(\delta)=-\tanh_{\varrho}\left(2\alpha\delta\right)\pm i\sqrt{mn}sech_{\varrho}\left(2\alpha\delta\right), \tag{3. 72}$$

$$\mathbb{Z}_{29}(\delta)=-\cot_{\varrho}\left(2\alpha\delta\right)\pm\sqrt{mn}\,csch_{\varrho}\left(2\alpha\delta\right), \tag{3. 73}$$

$$\mathbb{Z}_{30}(\delta)=-\frac{1}{2}\Bigg(\tanh_{\varrho}\left(\frac{\alpha}{2}\delta\right)+\coth_{\varrho}\left(\frac{\alpha}{2}\delta\right)\Bigg). \tag{3. 74}$$

Group 7: When $ß^2=4\alpha\ell$,

$$\mathbb{Z}_{31}(\delta)=\frac{-2\alpha(ß\delta\ln[\varrho]+2)}{ß^2\delta\ln[\varrho]}. \tag{3. 75}$$

Group 8: When $\alpha=pq,(q\neq 0),ß=p$, and $\ell=0$,

$$\mathbb{Z}_{32}(\delta)=\varrho^{p\delta}-q. \tag{3. 76}$$

Group 9: When $ß=\ell=0$,

$$\mathbb{Z}_{33}(\delta)=\alpha\delta\ln[\varrho]. \tag{3. 77}$$

Group 10: When $ß=\alpha=0$,

$$\mathbb{Z}_{34}(\delta)=\frac{-1}{\ell\delta\ln[\varrho]}. \tag{3. 78}$$

Group 11: When $\alpha=0$ and $ß\neq 0$,

$$\mathbb{Z}_{35}(\delta)=-\frac{mß}{\ell\left(\cosh_{\varrho}\left(ß\delta\right)-\sinh_{\varrho}\left(ß\delta\right)+m\right)}, \tag{3. 79}$$

$$\mathbb{Z}_{36}(\delta)=-\frac{ß\left(\sinh_{\varrho}\left(ß\delta\right)+\cosh_{\varrho}\left(ß\delta\right)\right)}{\ell\left(\sinh_{\varrho}\left(ß\delta\right)+\cosh_{\varrho}\left(ß\delta\right)+n\right)}. \tag{3. 80}$$

Group 12: When $\ell=pq,\ (q\neq 0),\ ß=p$, and $\alpha=0$,

$$\mathbb{Z}_{37}(\delta)=-\frac{m\varrho^{p\delta}}{m-qn\varrho^{p\delta}}, \tag{3. 81}$$

$$\sinh_{\varrho}(\delta)=\frac{m\varrho^{\delta}-n\varrho^{-\delta}}{2},\ \cosh_{\varrho}(\delta)=\frac{m\varrho^{\delta}+n\varrho^{-\delta}}{2},$$

$$\tanh_{\varrho}(\delta)=\frac{m\varrho^{\delta}-n\varrho^{-\delta}}{m\varrho^{\delta}+n\varrho^{-\delta}},\ \coth_{\varrho}(\delta)=\frac{m\varrho^{\delta}+n\varrho^{-\delta}}{m\varrho^{\delta}-n\varrho^{-\delta}},$$

$$sech_{\varrho}(\delta)=\frac{2}{m\varrho^{\delta}+n\varrho^{-\delta}},\ csch_{\varrho}(\delta)=\frac{2}{m\varrho^{\delta}-n\varrho^{-\delta}},$$

$$sin_{\varrho}(\delta)=\frac{m\varrho^{i\delta}-n\varrho^{-i\delta}}{2i},\ \ cos_{\varrho}(\delta)=\frac{m\varrho^{i\delta}+n\varrho^{-i\delta}}{2},$$

$$\tan_{\varrho}(\delta)=-i\frac{m\varrho^{i\delta}-n\varrho^{-i\delta}}{m\varrho^{i\delta}+n\varrho^{-i\delta}},\ \cot_{\varrho}(\delta)=i\frac{m\kappa^{i\delta}+n\varrho^{-i\delta}}{m\varrho^{i\delta}-n\varrho^{-i\delta}},$$

where, $\mathfrak{X}=ß^2-4\alpha\ell$ and $m,n>0$ are variables experiencing constant deception.

3.2.1. *Application of new extended direct algebraic method.* There is an assumed new expanded direct algebraic method. To generate a traveling wave transformation to obtain effects of Eq. (2. 1).

$$\mathbf{F}(x,t)=\mathbb{K}(\delta),\ \delta=x+\epsilon_0 y-\epsilon_1 t. \tag{3. 82}$$

Utilizing the formerly mentioned travelling wave transformation inside Eq. (3. 2), and get the ODE,

$$\epsilon_0\left(\epsilon_1^2-1\right)\mathbb{K}^{''}-2\epsilon_1\mathbb{K}^3-Q\mathbb{K}=0. \tag{3. 83}$$

By using the balancing rule $\mathbb{K}^3$ and $\mathbb{K}^{''}$ to get $J=1$, so the predicted solution in Eq.(3. 5) is truncated as,

$$\mathbb{K}(\delta)=a_0+a_1\mathbb{Z}(\delta). \tag{3. 84}$$

Next, put the solution from Eq. (3. 84) into Eq. (3. 83) and calculate the coefficients for the various powers.

$$\begin{aligned}
&\mathbb{Z}(\delta)^{\mathbf{0}}:\epsilon_0 a_1 ß\left(\ln(\varrho)\right)^2\alpha\,{\epsilon_1}^2-\epsilon_0 a_1 ß\left(\ln(\varrho)\right)^2\alpha-2,\ \epsilon_1\,{a_0}^3-Qa_0,\\
&\mathbb{Z}(\delta)^{\mathbf{1}}:\epsilon_0 a_1 ß^2\left(\ln(\varrho)\right)^2{\epsilon_1}^2-\epsilon_0 a_1 ß^2\left(\ln(\varrho)\right)^2+2\,\epsilon_0 a_1\ell\left(\ln(\varrho)\right)^2\alpha\,{\epsilon_1}^2-2\,\epsilon_0 a_1\ell\left(\ln(\varrho)\right)^2\alpha\\
&-6\,\epsilon_1\,{a_0}^2 a_1-Qa_1,\\
&\mathbb{Z}(\delta)^{\mathbf{2}}:3\,\epsilon_0 a_1 ß\left(\ln(\varrho)\right)^2\ell\,{\epsilon_1}^2-3\,\epsilon_0 a_1 ß\left(\ln(\varrho)\right)^2\ell-6\,\epsilon_0\,a_0 {a_1}^2,\\
&\mathbb{Z}(\delta)^{\mathbf{3}}:2\,\epsilon_0 a_1\ell^2\ln(\varrho)^2{\epsilon_1}^2-2\,\epsilon_0 a_1\ell^2\ln(\varrho)^2-2\,\epsilon_1\,{a_1}^3.
\end{aligned} \tag{3. 85}$$

The system explained in Eq.(3. 85) is solved with the help of the `Mathematica`.

Class 1:

$$\left[a_1=\pm 2\iota\sqrt{\frac{Q}{2\epsilon_1\mathfrak{X}}}\ell,a_0=\pm\iota\sqrt{\frac{Q}{2\epsilon_1\mathfrak{X}}}ß,\ \epsilon_0=\frac{2Q}{\mathfrak{X}\ln\varrho^2(1-\epsilon_1^2)}\right]. \tag{3. 86}$$

To obtain the general solution for Eq.(2. 1), insert Eq.(3. 86) into Eq. (3. 84):

$$\mathbb{K}(x,y,t) = \pm\iota\sqrt{\frac{Q}{2\epsilon_1\mathfrak{X}}}\text{ß} \pm 2\iota\sqrt{\frac{Q}{2\epsilon_1\mathfrak{X}}}\ell[\mathbb{Z}(\delta)], \tag{3. 87}$$

where,

$$\mathfrak{X} = \text{ß}^2 - 4\alpha\ell. \tag{3. 88}$$

To decide on solutions for the use of (NEAM), we consciousness entirely on the primary set and punctiliously discover all answers in diverse cases as defined below:

Set 1: If $\text{ß}^2 - 4\alpha\ell < 0$, and $\ell \neq 0$, the following describes how mixed trigonometric solutions are formed.

$$\mathbb{K}_1(x,y,t) = \mp\sqrt{\frac{Q}{2\epsilon_1}}\tan_\varrho\left(\frac{\sqrt{-\mathfrak{X}}}{2}(x+\epsilon_0 y-\epsilon_1 t)\right), \tag{3. 89}$$

$$\mathbb{K}_2(x,y,t) = \pm\sqrt{\frac{Q}{2\epsilon_1}}\cot_\varrho\left(\frac{\sqrt{-\mathfrak{X}}}{2}(x+\epsilon_0 y-\epsilon_1 t)\right), \tag{3. 90}$$

$$\begin{aligned}\mathbb{K}_3(x,y,t) = &\mp\sqrt{\frac{Q}{2\epsilon_1}}\Bigg(\tan_\varrho\left(\sqrt{-\mathfrak{X}}(x+\epsilon_0 y-\epsilon_1 t)\right)\\ &\pm\sqrt{mn}\sec_\varrho\left(\sqrt{-\mathfrak{X}}(x+\epsilon_0 y-\epsilon_1 t)\right)\Bigg),\end{aligned} \tag{3. 91}$$

$$\begin{aligned}\mathbb{K}_4(x,y,t) = &\mp\sqrt{\frac{Q}{2\epsilon_1}}\Bigg(\cot_\varrho\left(\sqrt{-\mathfrak{X}}(x+\epsilon_0 y-\epsilon_1 t)\right)\\ &\pm\sqrt{mn}\csc_\varrho\left(\sqrt{-\mathfrak{X}}(x+\epsilon_0 y-\epsilon_1 t)\right)\Bigg),\end{aligned} \tag{3. 92}$$

$$\begin{aligned}\mathbb{K}_5(x,y,t) = &\mp\frac{1}{2}\sqrt{\frac{Q}{2\epsilon_1}}\Bigg(\tan_\varrho\left(\frac{\sqrt{-\mathfrak{X}}}{4}(x+\epsilon_0 y-\epsilon_1 t)\right)\\ &-\cot_\varrho\left(\frac{\sqrt{-\mathfrak{X}}}{4}(x+\epsilon_0 y-\epsilon_1 t)\right)\Bigg).\end{aligned} \tag{3. 93}$$

Set 2: If $\text{ß}^2 - 4\alpha\ell > 0$, and $\ell \neq 0$, the obtain solutions in the various forms mentioned below.

When a shock solution is obtain as,

$$\mathbb{K}_6(x,y,t) = \mp\iota\sqrt{\frac{Q}{2\epsilon_1}}\left(\tanh_\varrho\left(\frac{\sqrt{\mathfrak{X}}}{2}(x+\epsilon_0 y-\epsilon_1 t)\right)\right). \tag{3. 94}$$

Accordingly, the singular solution is,

$$\mathbb{K}_7(x,y,t) = \mp\iota\sqrt{\frac{Q}{2\epsilon_1}}\left(\coth_\varrho\left(\frac{\sqrt{\mathfrak{X}}}{2}(x+\epsilon_0 y-\epsilon_1 t)\right)\right). \tag{3. 95}$$

To find a complex mixed solitary wave solution,

$$\begin{aligned}\mathbb{K}_8(x,y,t) = \pm\iota\sqrt{\frac{Q}{2\epsilon_1}}\Big(&-\tanh_\varrho\left(\sqrt{\mathfrak{X}}\,(x+\epsilon_0 y-\epsilon_1 t)\right)\\ &\pm i\sqrt{mn}_\varrho\left(\sqrt{\mathfrak{X}}\,(x+\epsilon_0 y-\epsilon_1 t)\right)\Big).\end{aligned} \tag{3. 96}$$

This is the method used to obtain the mixed singular result,

$$\begin{aligned}\mathbb{K}_9(x,y,t) = \pm\iota\sqrt{\frac{Q}{2\epsilon_1}}\Big(&-\coth_\varrho\left(\sqrt{\mathfrak{X}}\,(x+\epsilon_0 y-\epsilon_1 t)\right)\\ &\pm\sqrt{mn}_\varrho\left(\sqrt{\mathfrak{X}}\,(x+\epsilon_0 y-\epsilon_1 t)\right)\Big).\end{aligned} \tag{3. 97}$$

We get mixed shock singular solutions in the following format,

$$\begin{aligned}\mathbb{K}_{10}(x,y,t) = \mp\frac{\iota}{2}\sqrt{\frac{Q}{2\epsilon_1}}\Bigg(&\tanh_\varrho\left(\frac{\sqrt{\mathfrak{X}}}{4}\,(x+\epsilon_0 y-\epsilon_1 t)\right)\\ &+\coth_\varrho\left(\frac{\sqrt{\mathfrak{X}}}{4}\left(x+\epsilon_0 y-\epsilon_1 t\right)\right)\Bigg),\end{aligned} \tag{3. 98}$$

Set 3: If $\alpha\ell > 0$ and $ß = 0$, In the form of trigonometric expressions, we have the solution,

$$\mathbb{K}_{11}(x,y,t) = \pm\sqrt{\frac{Q}{2\epsilon}}\tan_\varrho\left(\sqrt{\alpha\ell}\,(x+\epsilon_0 y-\epsilon_1 t)\right), \tag{3. 99}$$

$$\mathbb{K}_{12}(x,y,t) = \mp\sqrt{\frac{Q}{2\epsilon}}\cot_\varrho\left(\sqrt{\alpha\ell}\,(x+\epsilon_0 y-\epsilon_1 t)\right). \tag{3. 100}$$

These solutions initiate the mixed trigonometric solutions,

$$\begin{aligned}\mathbb{K}_{13}(x,y,t) = \pm\sqrt{\frac{Q}{2\epsilon_1}}\Big(&\tan_\varrho\left(2\sqrt{\alpha\ell}\,(x+\epsilon_0 y-\epsilon_1 t)\right)\\ &\pm\sqrt{mn}\sec_\varrho\left(2\sqrt{\alpha\ell}\,(x+\epsilon_0 y-\epsilon_1 t)\right)\Big),\end{aligned} \tag{3. 101}$$

$$\begin{aligned}\mathbb{K}_{14}(x,y,t) = \pm\sqrt{\frac{Q}{2\epsilon_1}}\Big(&-\cot_\varrho\left(2\sqrt{\alpha\ell}\,(x+\epsilon_0 y-\epsilon_1 t)\right)\\ &\pm\sqrt{mn}\csc_\varrho\left(2\sqrt{\alpha\ell}\,(x+\epsilon_0 y-\epsilon_1 t)\right)\Big),\end{aligned} \tag{3. 102}$$

$$\begin{aligned}\mathbb{K}_{15}(x,y,t) = \pm\frac{1}{2}\sqrt{\frac{Q}{2\epsilon_1}}\Bigg(&\tan_\varrho\left(\frac{\sqrt{\alpha\ell}}{2}\,(x+\epsilon_0 y-\epsilon_1 t)\right)\\ &-\cot_\varrho\left(\frac{\sqrt{\alpha\ell}}{2}\,(x+\epsilon_0 y-\epsilon_1 t)\right)\Bigg).\end{aligned} \tag{3. 103}$$

Set 4: If $\alpha\ell < 0$ and $ß = 0$, we obtain solutions identified in the form of shock solutions,

$$\mathbb{K}_{16}(x,y,t) = \pm\sqrt{\frac{Q}{2\epsilon_1}}\tanh_\varrho\left(\sqrt{-\alpha\ell}\,(x+\epsilon_0 y-\epsilon_1 t)\right), \tag{3. 104}$$

The way to obtain the unique solution is as follows,

$$\mathbb{K}_{17}(x,y,t) = \pm\sqrt{\frac{Q}{2\epsilon_1}}\coth_\varrho\left(\sqrt{-\alpha\ell}\,(x+\epsilon_0 y-\epsilon_1 t)\right), \tag{3. 105}$$

The unique solutions for complex combinations are generated as,

$$\begin{aligned}\mathbb{K}_{18}(x,y,t) &= \pm\sqrt{\frac{Q}{2\epsilon_1}}\Big(-\tanh_\varrho\left(2\sqrt{-\alpha\ell}\,(x+\epsilon_0 y-\epsilon_1 t)\right)\\ &\pm i\sqrt{mn}_\varrho\left(2\sqrt{-\alpha\ell}\,(x+\epsilon_0 y-\epsilon_1 t)\right)\Big),\end{aligned} \tag{3. 106}$$

$$\begin{aligned}\mathbb{K}_{19}(x,y,t) &= \pm\sqrt{\frac{Q}{2\epsilon_1}}\Bigg(-\coth_\varrho\left(2\sqrt{-\alpha\ell}\,(x+\epsilon_0 y-\epsilon_1 t)\right)\\ &\pm\sqrt{mn}_\varrho\left(2\sqrt{-\alpha\ell}\,(x+\epsilon_0 y-\epsilon_1 t)\right)\Bigg),\end{aligned} \tag{3. 107}$$

$$\begin{aligned}\mathbb{K}_{20}(x,y,t) &= \pm\frac{1}{2}\sqrt{\frac{Q}{2\epsilon_1}}\Bigg(\tanh_\varrho\left(\frac{\sqrt{-\alpha\ell}}{2}\,(x+\epsilon_0 y-\epsilon_1 t)\right)\\ &+\coth_\varrho\left(\frac{\sqrt{-\alpha\ell}}{2}\,(x+\epsilon_0 y-\epsilon_1 t)\right)\Bigg).\end{aligned} \tag{3. 108}$$

Set 5: If $ß = 0$ and $\alpha = \ell$, we examine periodic and mixed periodic set solutions by analysing the category of periodic and mixed periodic solutions,

$$\mathbb{K}_{21}(x,y,t) = \pm\sqrt{\frac{Q}{2\epsilon}}\left(\tan_\varrho\left(\ell\,(x+\epsilon_0 y-\epsilon_1 t)\right)\right), \tag{3. 109}$$

$$\mathbb{K}_{22}(x,y,t) = \mp\sqrt{\frac{Q}{2\epsilon_1}}\left(\cot_\varrho\left(\ell\,(x+\epsilon_0 y-\epsilon_1 t)\right)\right), \tag{3. 110}$$

$$\begin{aligned}\mathbb{K}_{23}(x,y,t) &= \pm\sqrt{\frac{Q}{2\epsilon_1}}\Bigg(\tan_\varrho\left(2\ell\,(x+\epsilon_0 y-\epsilon_1 t)\right)\\ &\pm\sqrt{mn}\sec_\varrho\left(2\ell\,(x+\epsilon_0 y-\epsilon_1 t)\right)\Bigg),\end{aligned} \tag{3. 111}$$

$$\begin{aligned}\mathbb{K}_{24}(x,y,t) &= \pm\sqrt{\frac{Q}{2\epsilon_1}}\Bigg(-\cot_\varrho\left(2\ell\,(x+\epsilon_0 y-\epsilon_1 t)\right)\\ &\pm\sqrt{mn}\csc_\varrho\left(2\ell\,(x+\epsilon_0 y-\epsilon_1 t)\right)\Bigg),\end{aligned} \tag{3. 112}$$

$$\mathbb{K}_{25}(x,y,t) = \pm\frac{1}{2}\sqrt{\frac{Q}{2\epsilon_1}}\Bigg(\tan_\varrho\left(\frac{\ell}{2}\left(x+\epsilon_0 y-\epsilon_1 t\right)\right) - \cot_\varrho\left(\frac{\ell}{2}\left(x+\epsilon_0 y-\epsilon_1 t\right)\right)\Bigg). \tag{3. 113}$$

Set 6: If $ß = 0$ and $\ell = -\alpha$, to produce the single and mixed-wave compositions in the following category,

$$\mathbb{K}_{26}(x,y,t) = \pm\iota\sqrt{\frac{Q}{2\epsilon_1}}\tanh_\varrho\left(\alpha\left(x+\epsilon_0 y-\epsilon_1 t\right)\right), \tag{3. 114}$$

$$\mathbb{K}_{27}(x,y,t) = \pm\iota\sqrt{\frac{Q}{2\epsilon_1}}\coth_\varrho\left(\alpha\left(x+\epsilon_0 y-\epsilon_1 t\right)\right), \tag{3. 115}$$

$$\mathbb{K}_{28}(x,y,t) = \mp\iota\sqrt{\frac{Q}{2\epsilon_1}}\Bigg(-\tanh_\varrho\left(2\alpha\left(x+\epsilon_0 y-\epsilon_1 t\right)\right) \pm i\sqrt{mn}_\varrho\left(2\alpha\left(x+\epsilon_0 y-\epsilon_1 t\right)\right)\Bigg), \tag{3. 116}$$

$$\mathbb{K}_{29}(x,y,t) = \mp\iota\sqrt{\frac{Q}{2\epsilon_1}}\Bigg(-\cot_\varrho\left(2\alpha\left(x+\epsilon_0 y-\epsilon_1 t\right)\right) \pm \sqrt{mn}_\varrho\left(2\alpha\left(x+\epsilon_0 y-\epsilon_1 t\right)\right)\Bigg), \tag{3. 117}$$

$$\mathbb{K}_{30}(x,y,t) = \pm\frac{\iota}{2}\sqrt{\frac{Q}{2\epsilon_1}}\Bigg(\tanh_\varrho\left(\frac{\alpha}{2}\left(x+\epsilon_0 y-\epsilon_1 t\right)\right) + \coth_\varrho\left(\frac{\alpha}{2}\left(x+\epsilon_0 y-\epsilon_1 t\right)\right)\Bigg). \tag{3. 118}$$

The (**Set 7**), (**Set 8**), (**Set 9**), and (**Set 10**) have constant results.

Set 11: If $\alpha = 0$, $ß \neq 0$, The following gives the mixed hyperbolic solution,

$$\mathbb{K}_{35}(x,y,t) = \pm\iota\sqrt{\frac{Q}{2\epsilon_1}} \left[1-\left(\frac{2m}{\ell\left(\cosh_\varrho\left(ß\left(x+\epsilon_0 y-\epsilon_1 t\right)\right)-\sinh_\varrho\left(ß\left(x+\epsilon_0 y-\epsilon_1 t\right)\right)+m\right)}\right)\right] \tag{3. 119}$$

$$\mathbb{K}_{36}(x,y,t) = \pm\iota\sqrt{\frac{Q}{2\epsilon_1}} \left[1-2\left(\frac{ß\left(\sinh_\varrho\left(ß\left(x+\epsilon_0 y-\epsilon_1 t\right)\right)+\cosh_\varrho\left(ß\left(x+\epsilon_0 y-\epsilon_1 t\right)\right)\right)}{\ell\left(\sinh_\varrho\left(ß\left(x+\epsilon_0 y-\epsilon_1 t\right)\right)+\cosh_\varrho\left(ß\left(x+\epsilon_0 y-\epsilon_1 t\right)\right)+n\right)}\right)\right], \tag{3. 120}$$

Set 12: If $\ell = pq,\ (q \neq 0),\ ß = p$, and $\alpha = 0$, In the following, we derive the plane solution,

$$\mathbb{K}_{37}(x,y,t) = \pm\iota\sqrt{\frac{Q}{2\epsilon_1}}\left[1-\left(\frac{2m\varrho^{p(x+\epsilon_0 y-\epsilon_1 t)}}{m-qn\varrho^{p(x+\epsilon_0 y-\epsilon_1 t)}}\right)\right]. \tag{3. 121}$$

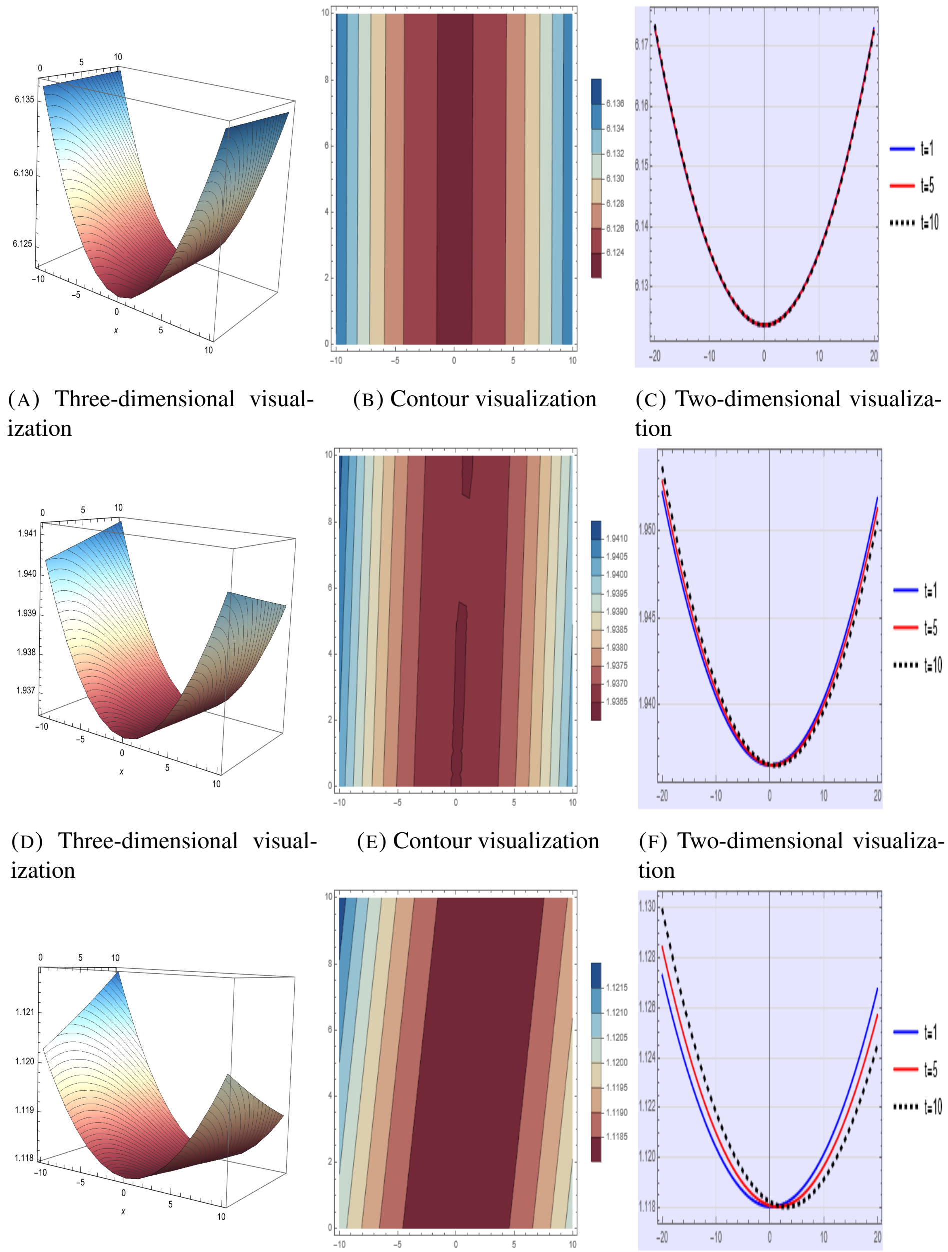

(A) Three-dimensional visualization

(B) Contour visualization

(C) Two-dimensional visualization

(D) Three-dimensional visualization

(E) Contour visualization

(F) Two-dimensional visualization

(G) Three-dimensional visualization

(H) Contour visualization

(I) Two-dimensional visualization

FIGURE 3. $\mathbb{K}_{18}(x,t)$ visual representations of the solution are provided in contour plots, two dimensions (2D), and three dimensions (3D).

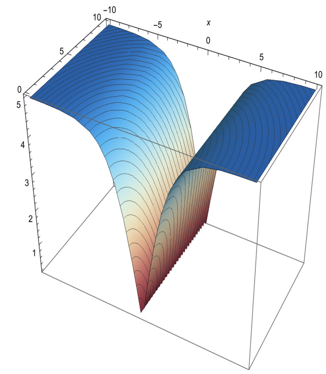

(A) Three-dimensional visualization

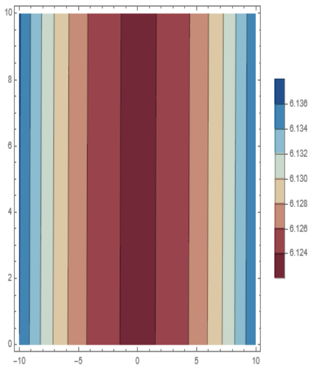

(B) Contour visualization

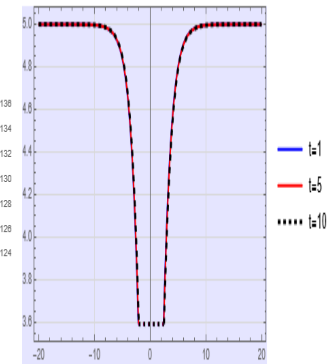

(C) Two-dimensional visualization

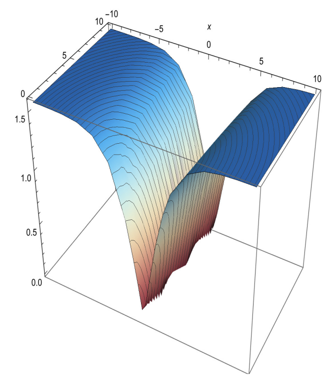

(D) Three-dimensional visualization

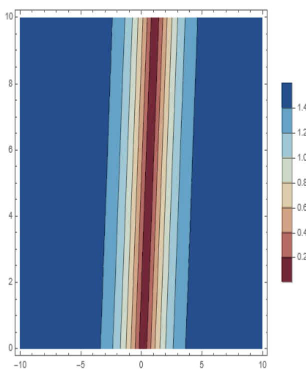

(E) Contour visualization

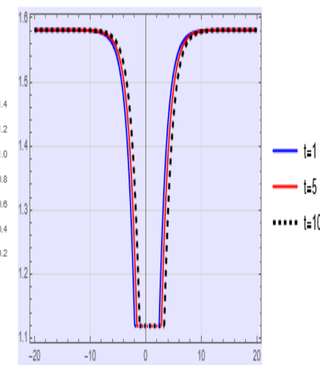

(F) Two-dimensional visualization

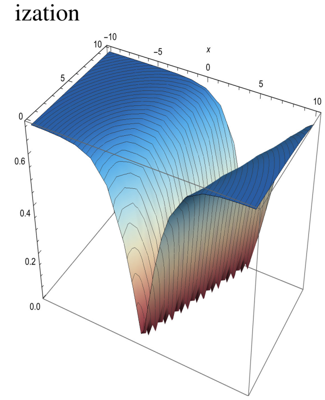

(G) Three-dimensional visualization

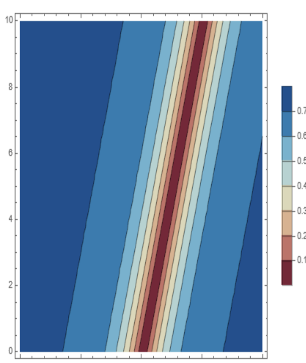

(H) Contour visualization

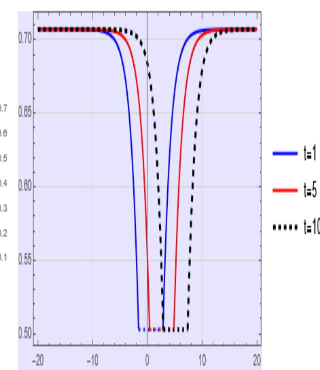

(I) Two-dimensional visualization

FIGURE 4. $\mathbb{K}_{35}(x,t)$ visual solutions are provided in two dimensions (2D), three dimensions (3D), and contour plots..

4. RESULTS AND DISCUSSION

The researchers examined the most notable applications of the (2+1)-D Zoomeron Model. The Sardar sub-equation method and the new extended direct algebraic method will find considerable value in the results of this paper.

Figure. 1 represents the composite multi-crested solutions with decay and bright soliton at variation in $e_1 = 0.6$, $e_1 = 0.06$, and $e_1 = 0.006$ and fixed the values $e_0 = 0.2$, $F = 0.3$, $p = 0.1$, and $q = 0.1$. For more visualization, contour plots and 3D, while 2D shows a soliton solution. These solutions describe wave packets that initially form multiple crests but gradually diminish in amplitude over time, resembling energy dissipation in optical fibers or plasma waves, where nonlinearity and dispersion balance each other.

Figure. 2 represents the periodic solitary wave with different amplitude, by changing the values of $e_0 = 0.009$, $e_0 = 0.09$, $e_0 = 0.9$ and fixed the values $e_0 = 0.7$, $F = 0.7$, $p = 0.1$, and $q = 0.1$. For more visualization, contour plots, in 3D, while 2D shows a soliton solution. Periodic solitary waves with different amplitudes, appear in fluid dynamics and nonlinear optics. These waves maintain a repetitive oscillatory pattern and can model water waves in deep oceans or light pulses in photonic devices.

Figure. 3 illustrates the flat kink behavior of soliton solution with the parametric values $\alpha = 0.001$, $l = 0.01$, $n = 0.3$, $m = 0.5$, $Q = 5$, at wave velocity $\epsilon_1 = 0.01$, as increasing the value of wave velocity same behavior can be seen. For more visualization, contour plots and bright soliton can be seen, while 2D shows a bright singular soliton solution. Kink behavior of soliton solutions, which represents a topological wave transition between two distinct states. Such structures are observed in magnetic domain walls, Bose-Einstein condensates, and signal propagation in nerve fibers.

Figure. 4 illustrates the anti-bell-shaped soliton structure with parametric values $\beta = 0.8$, $Q = 0.5$, $m = 0.9$, $Q = 5$ by increasing the wave velocity, the same behavior is observed, and the contour shows a dark soliton while 2D shows a dark singular soliton. These structures can be related to dark solitons in optical media, electron density depletion in plasmas, or structural deformations in solid-state materials.

The (2+1)-dimensional Zoomeron equation plays a crucial role in explaining wave behavior in disciplines such as material physics, optics, and acoustics, where understanding nonlinear interactions is essential. The visual representations generated in this study offer critical insights into these complex wave phenomena, aiding in the interpretation of soliton structures and their potential applications. These graphical depictions not only enhance our comprehension of nonlinear wave mechanics but also provide a foundation for developing advanced technologies in wave-based communication, laser pulse shaping, and energy transport systems.

Comparison of different solution types obtained in this study using the Sardar sub-equation approach and the new extended direct algebraic method.

TABLE 1. Comparison of obtained solutions.

Methods	Solution Type	Characteristics
Sardar Sub-Equation Approach	Composite multi-crested solutions with decay and bright soliton	Localized, decaying at infinity
Sardar Sub-Equation Approach	Periodic solitary wave with different amplitude	Oscillatory with varying amplitudes
New extended direct algebraic method	Flat kink soliton	Smooth transition between two states
New extended direct algebraic method	Anti-bell-shaped soliton	Inverted profile of flat kink

TABLE 2. Comparison of obtained solutions with previously reported results in the literature.

Reference	Method	Solutions
Ullah et. al [34]	Extended Jacobian elliptic function	Bright-dark breather waves Singular breather waves
Yang et. al [36]	Modified rational expansion method	Bright soliton Dark soliton Periodic soliton
Batool et. al [9]	$(\frac{G'}{G^2})$-expansion method	Exact solutions
Zeng et. al [42]	New extended auxiliary equation approach	Singular soliton Periodic soliton
Novelty in This Work	SSEM NEDAM	New interaction patterns and wave structures Introduced anti-flat kink and decay soliton solutions

5. CONCLUSION

In this study, the Sardar sub-equation approach and a new extended direct algebraic method are employed to investigate the (2+1)-dimensional Zoomeron model equation, yielding a diverse set of solitary and traveling wave solutions. The accuracy of the obtained results is rigorously verified using the computational software `Mathematica`. The findings underscore the reliability and efficiency of both methodologies. The study reveals a variety of novel wave structures, including anti-peaked decay solitons, periodic solitary waves with varying amplitudes, flat kink solutions, and anti-flat kink solutions. These results provide valuable insights into nonlinear wave behavior, with significant implications for applications in optics, fluid dynamics, and material science.

A key contribution of this work is the application of the new extended direct algebraic method to the study of obliquely interacting surface waves, offering a fresh perspective on nonlinear wave interactions. The graphical representations presented through 3D, 2D, and contour plots further enhance the comprehension of these intricate waveforms, contributing to both theoretical and applied research in wave propagation phenomena. Future research may extend these methodologies to fractional-order nonlinear equations, facilitating the study of nonlocal and memory-dependent systems. Additionally, exploring multi-soliton interactions and collision dynamics within the framework of the Zoomeron model presents an exciting avenue for further investigation.

Acknowledgments. All the authors are obliged and thankful to the University of Lahore, Pakistan, for facilitating and supporting the research work.

Authors' contributions

Formal analysis, problem formulation U.A and A.J; Investigation, Methodology M.I.A, A.J and U.A, Supervision, resources, validation, graphical discussion and software; U.A and M.A Review and editing; all authors approved the final version for submission.

Funding

No funding available.

Ethics approval and consent to participate

Not applicable

Consent for publication

Not applicable

Availability of data and material

Data sharing is not applicable to this article as no data sets were generated or analyzed during the current study.

Competing interests

The authors declare that they have no competing interests.

REFERENCES

[1] Z. Abbas, *Coupled Gerdjikov-Ivanov system and its exact solutions through Darboux transformation*, Punjab Univ. J. Math. **54**, No. 3 (2022)

[2] X. Ahmad, T. Mahmood, K. Ullah, and N. Jan, *Similarity measures based on the novel interval-valued picture hesitant fuzzy sets and their applications in pattern recognition*, Punjab Univ. J. Math. **54**, No. 7 (2022).

[3] K. K. Ali, S. A. AlQahtani, M. S. Mehanna,and A. Bekir, *New optical soliton solutions for the (2+ 1) Fokas system via three techniques*, Optical and Quantum Electronics, **55**, No. 7, (2023), 638.

[4] G. Arora, R. Rani, and H Emadifar, *Numerical solutions of nonlinear Schrodinger equation with applications in optical fiber communication*, Optik **266** (2022): 169661.

[5] G. Arora, R. Kumar, and H. Temimi. *An implicit semi-analytical technique: Development, analysis and applications*, Mathematics and Computers in Simulation **226** (2024): 500-510.

[6] U. Asghar, M. I. Asjad, W. A. Faridi, and T. Muhammad, *The conserved vectors and solitonic propagating wave patterns formation with Lie symmetry infinitesimal algebra*, Optical and Quantum Electronics **56**, No. 4 (2024): 540.

[7] U. Asghar, W. A. Faridi, M. I. Asjad, and S. M. Eldin, *The enhancement of energy-carrying capacity in liquid with gas bubbles, in terms of solitons*, Symmetry **14**, No. 11 (2022): 2294.

[8] M. Asma, *Optical Soliton Perturbation with Quadratic-Cubic Nonlinearity.* Diss. University of Malaya (Malaysia), 2020.

[9] F. Batool, G. Akram, M. Sadaf, and U. Mehmood, *Dynamics investigation and solitons formation for (2+ 1)-dimensional zoomeron equation and foam drainage equation*, Journal of Nonlinear Mathematical Physics **30**, No. 2 (2023): 628-645.

[10] S. Duran, A. Yokus, and G. Kilinc, *A study on solitary wave solutions for the Zoomeron equation supported by two-dimensional dynamics*, Physica Scripta **98**, No. 12 (2023): 125265.

[11] S. H. Duran, M. Yavuz, and A. Yokus, *Discussion of numerical and analytical techniques for the emerging fractional order murnaghan model in materials science*. Optical and Quantum Electronics **55**, No. 6, (2023): 571.

[12] W. A. Faridi, U. Asghar, M. I. Asjad, A. M. Zidan, and S. M. Eldin, *Explicit propagating electrostatic potential waves formation and dynamical assessment of generalized Kadomtsev–Petviashvili modified equal width-Burgers model with sensitivity and modulation instability gain spectrum visualization*, Results in Physics **44** (2023): 106167.

[13] O. G. Gaxiola, *Optical soliton solutions for Triki–Biswas equation by Kudryashov's R function method*, Optik **249** (2022): 168230.

[14] Y. Haiyang, W. Haiyan, Z. Zhichen, X. Yong, and J. Kurths. *A stochastic nonlinear differential propagation model for underwater acoustic propagation: Theory and solution*. Chaos, Solitons and Fractals **150** (2021): 111105.

[15] K. Hosseini, Z. Ayati, and R. Ansari, *New exact solutions of the Tzitzéica-type equations in non-linear optics using the exp a function method*, Journal of Modern Optics **65**, No. 7, (2018): 847-851.

[16] M. B. Hossen, H. O. Roshid, and M. Z. Ali, *Characteristics of the solitary waves and rogue waves with interaction phenomena in a (2+ 1)-dimensional Breaking Soliton equation*, Physics Letters A **382**, No. 19 (2018): 1268-1274.

[17] K. Iqbal, M. Zhang, S. Piao, and H. Ge. *Evolution of sonobuoy through history and its applications: A survey* In 2020 17th International Bhurban Conference on Applied Sciences and Technology (IBCAST), (2020) 543-554.

[18] V. Jadaun, S. Kumar, and Y. Garg, *Symmetry analysis and soliton solution of (2+ 1)-dimensional Zoomeron equation*, arXiv preprint arXiv: **1701**, (2017), 05499.

[19] A. Jhangeer, Beenish, A. M. Talafha, A. R. Ansari, and M. Imran. *Analytical and dynamical analysis of nonlinear Riemann wave equation in plasma systems*. Arab Journal of Basic and Applied Sciences **31**, No. 1 (2024): 536-553.

[20] A. Jhangeer, H. Ehsan, M. B. Riaz, and A. M. Talafha, *Impact of fractional and integer order derivatives on the (4+ 1)-dimensional fractional Davey–Stewartson–Kadomtsev–Petviashvili equation*, Partial Differential Equations in Applied Mathematics **12** (2024): 100966.

[21] S. Kumar, and S. Rani, *Lie symmetry reductions and dynamics of soliton solutions of (2+ 1)-dimensional Pavlov equation*. Pramana **94**, No. 1, (2020): 116.

[22] S. Lin, and Y. Chen, *Physics-informed neural network methods based on Miura transformations and discovery of new localized wave solutions*, Physica D: Nonlinear Phenomena **445** (2023): 133629.

[23] S.Y. Lou and H. C. Ma, *Non-Lie symmetry groups of (2+ 1)-dimensional nonlinear systems obtained from a simple direct method*. Journal of Physics A: Mathematical and General **38**, No. 7 (2005): L129.

[24] X. Lü, and S. J. Chen, *Interaction solutions to nonlinear partial differential equations via Hirota bilinear forms: one-lump-multi-stripe and one-lump-multi-soliton types*, Nonlinear Dynamics **103**, No. 1 (2021): 947-977

[25] W. X. Ma, *Inverse scattering and soliton solutions of nonlocal reverse-spacetime nonlinear Schrödinger equations*, Proceedings of the American Mathematical Society, **149**, No. 1 (2021) 251-263.

[26] V. G. Makhankov, Y. P. Rybakov, and V. I. Sanyuk. *The Skyrme Model: Fundamentals Methods Applications*. Springer Science and Business Media, 2012.

[27] B. A. Malomed, *Basic fractional nonlinear-wave models and solitons*, Chaos: An Interdisciplinary Journal of Nonlinear Science **34**, No. 2 (2024).

[28] M. N. Nawaz, Muhammad, *Cubic B-spline solution of nonlinear sixth order boundary value problems*, Punjab Univ. J. Math. **50**, No. 4 (2020).

[29] M. S. Osman, K. U. Tariq, A. Bekir, A. Elmoasry, N. S. Elazab, M. Younis, and M. A. Aty, *Investigation of soliton solutions with different wave structures to the (2+1)-dimensional Heisenberg ferromagnetic spin chain equation*, Communications in Theoretical Physics **72**, No. 3, (2020): 035002.

[30] M. Ozisik, A. Secer, and M. Bayram, *On solitary wave solutions for the extended nonlinear Schrödinger equation via the modified F-expansion method*, Optical and Quantum Electronics **55**, No. 3 (2023): 215.

[31] N. Raza, A. Jhangeer, Z. Amjad, B. Rani, and T. Muhammad, *Analyzing coupled-wave dynamics: lump, breather, two-wave and three-wave interactions in a (3+ 1)-dimensional generalized KdV equation*, Nonlinear Dynamics **112**, No. 24 (2024): 22323-22341.

[32] R. Silambarasan, and K. S. Nisar, *Doubly periodic solutions and non-topological solitons of (2+ 1)-dimension Wazwaz Kaur Boussinesq equation employing Jacobi elliptic function method*, Chaos, Solitons & Fractals **175** (2023): 113997.

[33] A. Silem, and J. Lin, *Exact solutions for a variable-coefficients nonisospectral nonlinear Schrödinger equation via Wronskian technique*, Applied Mathematics Letters 135 (2023): 108397.

[34] M. S. Ullah, H. O. Roshid, and M. Z. Ali, *New wave behaviors and stability analysis for the (2+ 1)-dimensional Zoomeron model*, Optical and Quantum Electronics, **56**, No. 2, (2024) 240.

[35] K. J. Wang, and J. Si, *Diverse optical solitons to the complex Ginzburg–Landau equation with Kerr law nonlinearity in the nonlinear optical fiber*, The European Physical Journal Plus **138**, No. 3 (2023): 187.

[36] L. Yang, M. U. Rahman, and M. A. Khan, *Complex dynamics, sensitivity analysis and soliton solutions in the (2+ 1)-dimensional nonlinear Zoomeron model*, Results in Physics **56**, (2024): 107261.

[37] S. W. Yao, G. Akram, M. Sadaf, I. Zainab, H. Rezazadeh, and M. Inc, *Bright, dark, periodic and kink solitary wave solutions of evolutionary Zoomeron equation*, Results in Physics **43** (2022): 106117.

[38] A. Yokuş, H. Durur, S. Duran, and M. T. Islam, *Ample felicitous wave structures for fractional foam drainage equation modeling for fluid-flow mechanism*. Computational and Applied Mathematics **41**, No. 4, (2022): 174.

[39] H. Yu, P. Li, L. Zhang, Y. Zhu, F. A. Al-Zahrani, and K. Ahmed. *Application of optical fiber nanotechnology in power communication transmission*. Alexandria Engineering Journal **59**, No. 6 (2020): 5019-5030.

[40] U. H. M. Zaman, *Utilizing the extended tanh-function technique to scrutinize fractional order nonlinear partial differential equations*, Partial Differential Equations in Applied Mathematics **8** (2023): 100563.

[41] E. M. Zayed, R. M. A. Shohib, and M. E. Alngar, *New extended generalized Kudryashov method for solving three nonlinear partial differential equations*, Nonlinear Analysis: Modelling and Control **25**, No. 4 (2020): 598-617.

[42] Z. Zeng, X. Liu, Y. Zhu, and X. Huang, *New exact traveling wave solutions of (2+ 1)-dimensional time-fractional zoomeron equation*, Journal of Applied Mathematics and Physics **10**, no. 2, (2022): 333-346.

[43] Q. Zhang, M. Xiong, and L. Chen. *Exact solutions of two nonlinear partial differential equations by the first integral method*, Advances in Pure Mathematics **10**, No. 1 (2020): 12.

[44] R. Zhang, S. Bilige, and T. Chaolu, *Fractal solitons, arbitrary function solutions, exact periodic wave and breathers for a nonlinear partial differential equation by using bilinear neural network method*, Journal of Systems Science and Complexity **34**, No. 1, (2021): 122-139.

[45] R. F. Zhang and M. C. Li, *Bilinear residual network method for solving the exactly explicit solutions of nonlinear evolution equations*, Nonlinear Dynamics **108**, No. 1, (2022): 521-531.

[46] R. F. Zhang, M. C. Li, J. Y. Gan, Q. Li, and Z. Z. Lan, *Novel trial functions and rogue waves of generalized breaking soliton equation via bilinear neural network method*, Chaos, Solitons & Fractals **154** (2022): 111692.